CHAPTER V
SYNTHESIS GAS PRODUCTION
IN CORONA DISCAHRGE OVER Pt/KL

5.1 Abstract

This study investigated the effects of electrical parameters of a corona discharge reactor on the partial oxidation of methane in air and on carbon dioxide reforming of methane in the presence and absence of Pt loaded KL zeolite (Pt/KL). The experiments were conducted over a wide range of applied frequency (200-800 Hz) and input low side voltage (32-72 V). For partial oxidation of methane, the reactant conversions increased with decreasing applied frequency and increased with input low side voltage both in the presence and absence of Pt/KL except that the oxygen conversion was 100% in the presence of Pt/KL. Compared to the corona discharge in the absence of Pt/KL, the presence of Pt/KL resulted in higher oxygen conversion but lower methane conversion. In the absence of Pt/KL, the CO/C_2 and H_2/CO ratios were constant of about 12 and 1.8 at high current but in the presence of Pt/KL the CO/C_2 and H_2/CO ratios both increased with decreasing applied frequency and increasing input low side voltage. For carbon dioxide reforming with methane, applied frequency and input low side voltage affected only reactant conversions with no significant effect on reaction pathways both in the presence and absence of Pt/KL. The combination of catalyst and corona discharge had no strong effect on carbon dioxide reforming with methane.

5.2 Introduction

Natural gas is a versatile energy resource containing methane as its main component. The conversion of methane to synthesis gas has a long history of commercial practice and remains the subject of much research. Synthesis gas is used as a feedstock in many industrial processes such as methanol synthesis and Fischer-Tropsch process. There are two main commercial routes for conversion of methane to synthesis gas: steam reforming (Reaction 5.1) and partial oxidation (Reaction 5.2).

There is also significant interest in carbon dioxide reforming (Reaction 5.3) for high carbon dioxide containing natural gas resources. These routes are described by the following stoichiometric equations, respectively.

$$CH_4 + H_2O \rightarrow CO + 3H_2 \quad (5.1)$$

$$CH_4 + 1/2\,O_2 \rightarrow CO + 2H_2 \quad (5.2)$$

$$CH_4 + CO_2 \rightarrow 2CO + 2H_2 \quad (5.3)$$

Steam reforming of methane is the well-known process for synthesis gas production. A typical industrial steam reformer operates at 1,120-1,170 K and 15-30 atm over a Ni/Al_2O_3 catalyst[1]. This strongly endothermic reaction requires very high heat fluxes provided in direct fired furnace tubes. The H_2/CO ratio is further adjusted by the water gas shift reaction by using iron oxide/chromia catalyst when hydrogen production is the objective. Hence, the disadvantages of steam reforming of methane are high cost and complicated process. Therefore, new processes that convert methane to syngas at the simpler condition is expected as the aim of this work.

The partial oxidation is an exothermic reaction that produces syngas with the ideal ratio for production of methanol or the Fischer-Tropch process. It also uses a smaller and simpler reactor and less energy than steam reforming[1]. While using air as a source of oxygen can reduce the synthesis gas production cost, however using cryogenically produced oxygen, though expensive, is common practice. However, total oxidation of methane has to be avoided as it produces water and carbon dioxide instead of the desired products.

Due to the fact that carbon dioxide is a major component in both greenhouse gases and many natural gas resources, especially in Asia, a potentially useful reaction for reducing the net impact of carbon dioxide is becoming increasing important. A number of research efforts have studied methane catalytic reforming with carbon dioxide to produce synthesis gas. Carbon dioxide reforming with methane has some advantages over steam reforming, such as producing a lower H_2/CO ratio when advantageous, and the possibility of producing higher purity carbon monoxide[2] but it is also highly endothermic and requires high heat fluxes. A major problem of carbon

dioxide reforming with methane, resulting from the high carbon content in the feed stream, is the high level of carbon deposition (Reactions 5.4 and 5.5), causing deactivation of the catalyst.

$$CH_4 \rightarrow C + 2H_2 \qquad (5.4)$$

$$2CO \rightarrow C + CO_2 \qquad (5.5)$$

A plasma is a quasineutral gas consisting of charged and neutral gas molecules with a collective behavior in which the charged molecules follow the path of the electric field. Historically, plasma chemistry technologies started as equilibrium plasma processes using plasma jets for heating. Later, it was found that the non-equilibrium plasma, non-thermal or cold plasma, has more benefits for initiating chemical reactions at low temperatures and with lower energy input, due to its non-equilibrium properties (The electron temperatures can reach to 10,000 – 100,000 K or 1-10 eV, while the bulk gas temperatures remain low.).

Recently, non-equilibrium plasmas have been extensively studied as a possible way to initiate the reaction of methane to various products, such as methanol and higher hydrocarbons for industrial application[3-9]. A number of researchers are also interested in finding a way to improve synthesis gas production from methane using electric discharge plasmas[8,10]. The corona discharge is one of the useful plasma reactor types due to its ease of operating at atmospheric pressure. Applications for corona discharge processes have existed for over a hundred years, and they play an important role in many industrial applications, such as electrostatic precipitation, electro photography, static control in semiconductor manufacture, ionization instrumentation, generation of ozone and destruction of toxic compounds[11, 12].

Methane conversion to acetylene in a DC corona discharge has been found in the presence of NaY zeolite since the electrostatic potential and/or work function of the catalyst were altered by charge accumulation on the catalyst surface[13]. It was also found that using NaX zeolite in the DBD could inhibit the formation of undesired solid carbonaceous species[14]. The combination of zeolite and plasma

could be an alternative way to improve synthesis gas production from methane. This study used a corona discharge to activate the partial oxidation of methane in air and the carbon dioxide reforming with methane to produce synthesis gas in the presence and absence of Pt/KL zeolite. The effects of applied frequency and input low side voltage on reactant conversions, H_2/CO ratio, and CO/C_2 ratio were investigated.

5.3 Experimental

5.3.1 Experimental Set up

The flow rates of feed gases were controlled by a set of mass flow controllers supplied by SIERRA Instrument, Inc. at a total flow rate of 50 sccm for all experiments corresponding to a residence time of about 0.78 s. The feed gases were introduced downward through the reactor and analyzed on-line by a Perkin-Elmer gas chromatograph with thermal conductivity (TCD) and flame ionization (FID) detectors. The exhaust gas from the reactor was introduced into a condenser cooled with a mixture of dry ice and acetone that was used to remove the condensable products. Water was not quantified. All experiments were carried out at atmospheric pressure. The power supply unit consisted of an AC power supply for converting domestic AC power 220 V, 50 Hz, using a function generator for varying the frequency with a sinusoidal waveform. The output was then transmitted to a high voltage alternating current (HVAC) transformer. The HVAC stepped up the low side voltage to the high side voltage by the nominal factor of 125 at 60 Hz. This factor may not be constant, with frequency due to changes in the power factor because of the capacitive nature of the reactor system. The electrodes were connected to the HVAC by stainless steel rods. The configuration of the reactor is shown in Figure 5.1. The discharge occurred in a quartz tube with an i.d. of 8 mm between two stainless steel electrodes. The upper wire electrode was centered axially within the reactor tube, while the lower electrode was a circular plate with eight holes to allow gas to pass through the reactor and was positioned perpendicular to the reactor axis. The gap distance between these two electrodes was 13 mm. The catalyst was packed in the reactor on the lower electrode with equal weight for every experiment of 0.08 g. The height of the catalyst bed was 5 mm. The gas discharge was usually initiated

at room temperature and the gas was self-heated by the plasma. A significant potential problem of using air as a source of oxygen in plasma systems is the formation of NO_x. The exhaust gas from partial oxidation in air experiments was tested by an NO_x analyzer (42 C NO-NO_2-NO_x, Thermo Environmental Instrument Inc.). NO_x was not detected.

For this system, the conversions are defined as:

Conversion of CH_4 = (moles of CH_4 consumed/moles of CH_4 introduced) × 100 %

Conversion of O_2 = (moles of O_2 consumed/moles of O_2 introduced) × 100 %

Conversion of CO_2 = (moles of CO_2 consumed/moles of CO_2 introduced) × 100 %

H_2/CO mole ratio = moles of H_2 produced/moles of CO produced

CO/C_2 mole ratio = moles of CO produced/moles of C_2H_2, C_2H_4 and C_2H_6 produced

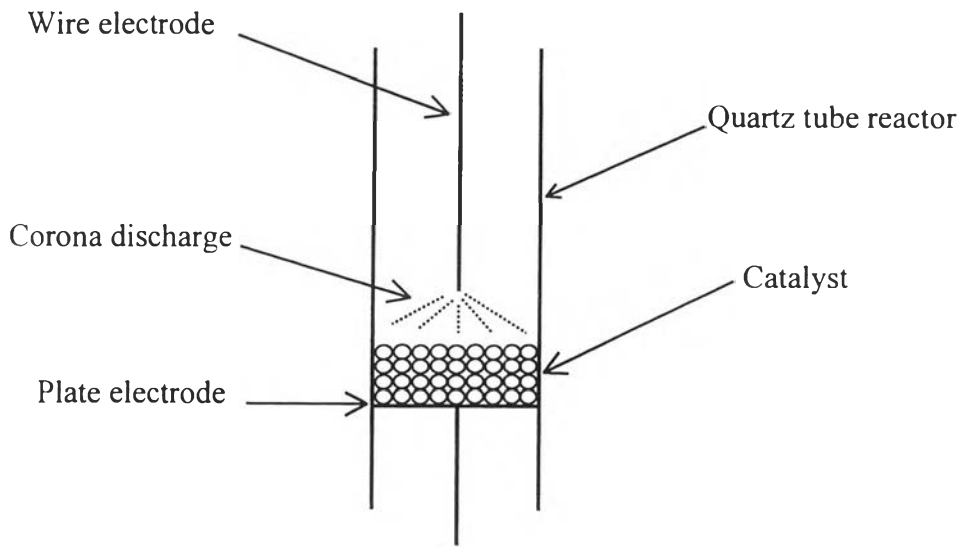

Figure 5.1 Corona discharge reactor configuration.

5.3.2 Catalyst Preparation

The catalysts were prepared at 1% wt loading of platinum (Pt) on KL zeolite supports. KL zeolite was prepared by drying in an oven at 110 °C overnight and calcining at 400 °C in dry air with a constant flow rate of 100 sccm/g of catalyst for 5 h with a temperature ramp of 3 °C/min. The incorporation of platinum metal

into the zeolite was performed using the chemical vapor deposition (CVD) method. Weighed platinum (II) acetylacetonate (Pt $(AcAc)_2$) was mixed physically with the dried zeolite under a nitrogen atmosphere. The mixture was loaded into a tube under a helium flow rate of 2 sccm. The mixture was slowly ramped to 40 °C and held there for 3 h, and then ramped again to 60 °C and held again for 1 h. The procedure was repeated by increasing temperature to 80, 90 and then 100 °C. After ramping to 100 °C, the mixture was held at that temperature for 1 h to sublime the $Pt(AcAc)_2$. After sublimation, the mixture was ramped to 130 °C and held for 15 minutes to ensure that virtually all of $Pt(AcAc)_2$ was sublimed. The reactor was cooled to room temperature, and the sample was removed. At this point, the sample was ramped to 350 °C in flowing air for 2 h and calcined at that temperature for 2 h to decompose the platinum precursor. The resultant Pt/KL catalyst was stored in a desiccator. The percentages of platinum on zeolites were analyzed by an atomic absorption spectrometer (Varian, SpectrAA-300). The analysis results of actual platinum loadings were 1.00%. Prior to reaction, the catalyst was reduced in situ in 1 sccm of H_2/mg of Pt/KL. The catalyst was ramped to 350 °C for 2 h and held at that temperature for 1 h.

5.4 Results and Discussion

Since the electrical parameters have been expressed as significant variables affecting the performance of the non-equilibrium plasma reactor[3,8,15,16], this work concentrated on the effects of applied frequency and input low side voltage on partial oxidation of methane in air and carbon dioxide reforming with methane in the presence and absence of Pt/KL.

To study the effects of electrical parameters on partial oxidation of methane in air, the CH_4/O_2 feed mole ratio was set at 2:1 with a residence time of 0.78 s. The effects of frequency on methane and oxygen conversions of partial oxidation reaction are shown in Figure 5.2. Methane conversion in the presence and absence of Pt/KL and oxygen conversion in the absence of Pt/KL decreased with increasing frequency, while oxygen conversion in the presence of Pt/KL was always 100%. In the presence of catalyst, the lowest applied frequency used was 400 Hz, but the

frequency could be decreased lower than 400 Hz in the absence of catalyst. The conversion of methane in the presence of the catalyst was lower than the one without catalyst. In contrast with methane conversion, the oxygen conversion in the presence of catalyst was higher than without catalyst. This means that in the presence of catalyst, oxygen was consumed by other side reactions and the conversion of methane was limited by the availability of oxygen, which was consumed completely. These behaviors were also found with the effects of input low side voltage on partial oxidation of methane in air, as show in Figure 5.3. The methane and oxygen conversions increased with increasing input low side voltage in the presence and absence of catalyst, except that the oxygen conversion in the presence of catalyst, which was again always 100%.

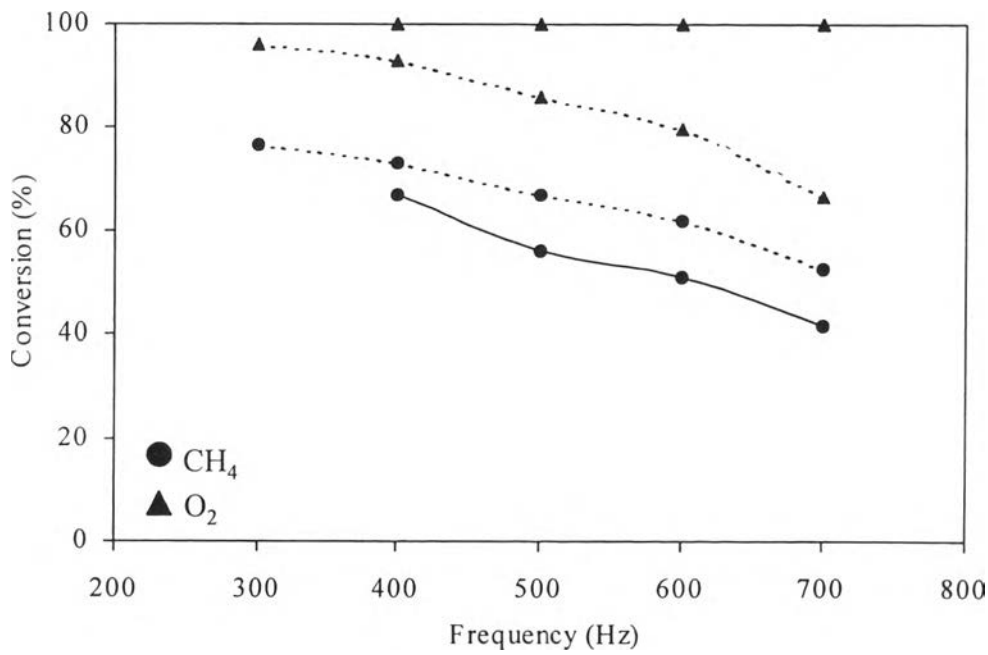

Figure 5.2 Effects of applied frequency on reactant conversions for methane partial oxidation in air; input low side voltage, 64 V and with (—)/without (---) Pt/KL.

The discharge was easier to establish in the presence of the catalyst, so the lowest input low side voltage in the presence of the catalyst was lower than without the catalyst. However, in the presence of the catalyst, carbon deposits were easier to form at both electrodes due to the rough surface of the catalyst. Consequently, in the

presence of the catalyst, the input low side voltage could not be increased as high as in the absence of the catalyst.

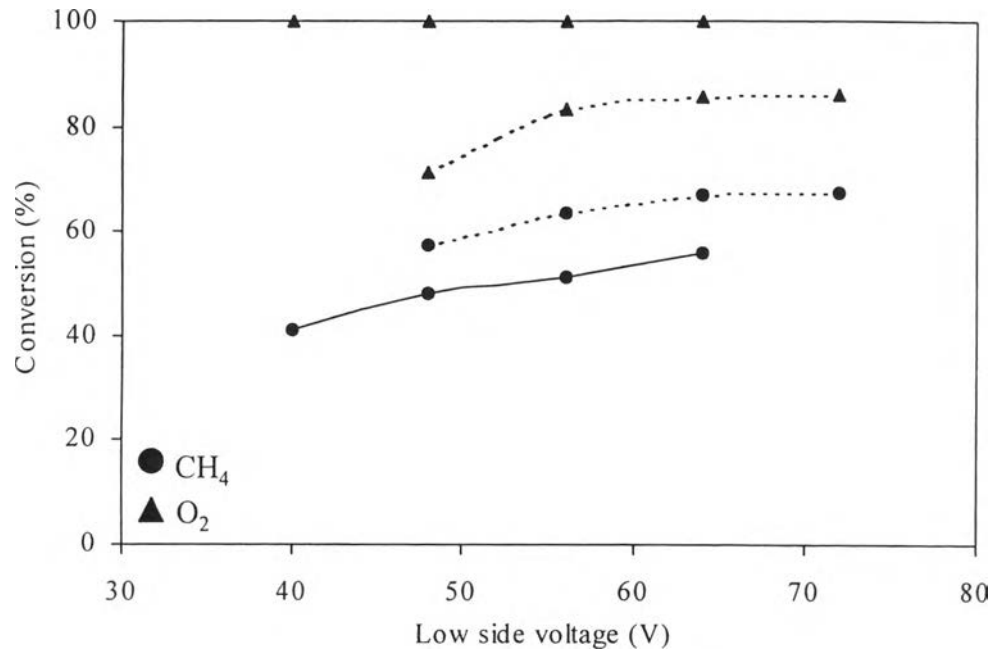

Figure 5.3 Effects of input low side voltage on reactant conversions for methane partial oxidation in air; applied frequency, 500 Hz and with (—)/without (---) Pt/KL.

The main effect of frequency on the conversions and product distribution is due to the space charge (electrons and ions) characteristics of the discharge. As the AC discharge is applied, each electrode performs alternatively as anode or cathode. The alternating behavior has proven effective in minimizing or eliminating contaminant accumulation on the electrodes which shows that the system behavior is significantly different between AC and DC discharge[16]. The space charge between the two electrodes is eliminated and then a new space charge is initiated every half cycle. With increasing frequency, a faster reversal of the electric field reduces the decay of the space charge. Acceleration of the remaining space charge by the reversing electric field can decrease the amount of current needed to sustain the discharge[17]. The capacitive nature of the reactor creates a phase lag between the voltage and current waveforms, and this increases with higher frequency, thus reducing the power factor and discharge power at constant applied voltage. For these

reasons, the current of the system decreases with increasing frequency, as shown in Figure 5.4.

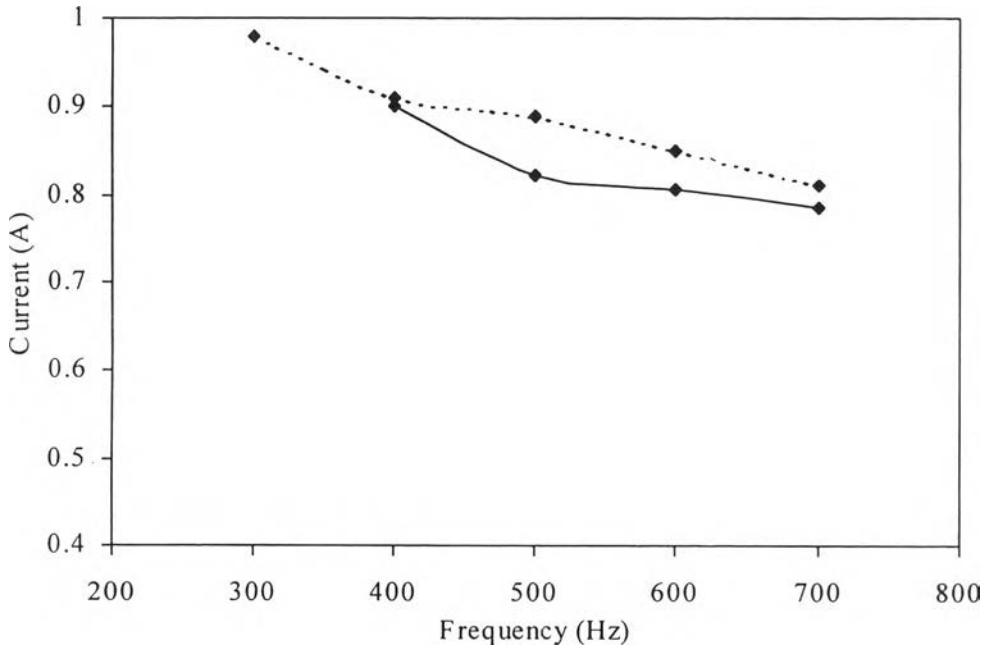

Figure 5.4 Effects of applied frequency on current for methane partial oxidation in air; input low side voltage, 64 V and with (—)/without (---) Pt/KL.

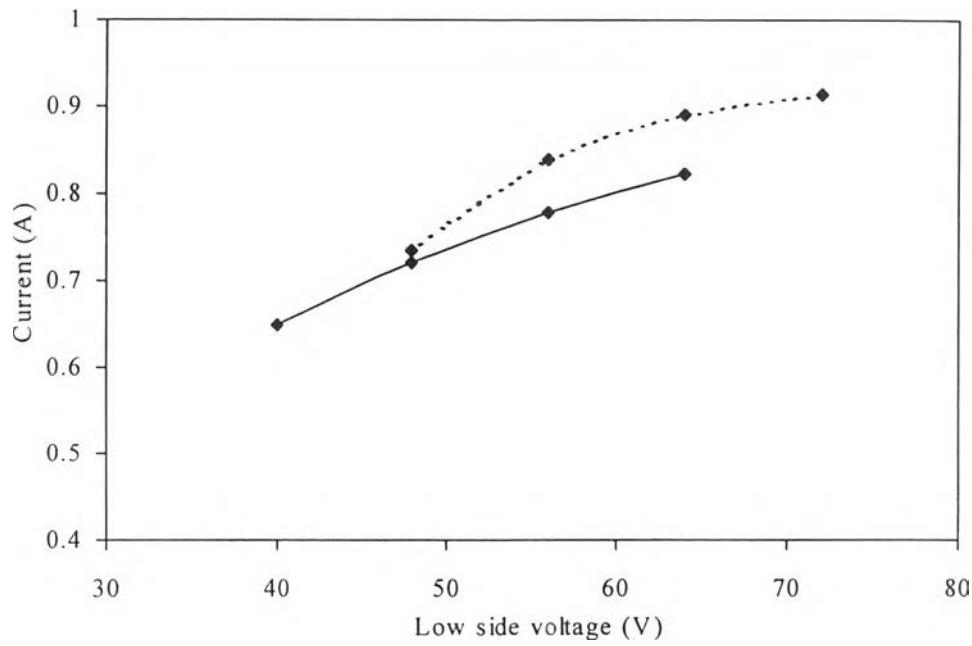

Figure 5.5 Effects of input low side voltage on current for methane partial oxidation in air; applied frequency, 500 Hz and with (—)/without (---) Pt/KL.

Increased voltages result in higher electric field strength, thereby promoting a higher average electron energy as confirmed by increasing current with increasing voltage, as shown in Figure 5.5. Morinaga and Suzuki also found that, with a fixed geometry, the quantity of electricity transferred between the electrodes increased, i.e. the current increased with increasing voltage[18,19]. The current decreased with increasing applied frequency and increased with input low side voltage, both with and without Pt/KL. The current of the system in the presence of Pt/KL was lower than the current in the absence of the catalyst. Since the number of available electrons to initiate the reaction increased with increasing current, methane and oxygen conversions increased with increasing current.

There are two main proposed reaction mechanisms for the partial catalytic oxidation of methane to synthesis gas[1,20]. First, the combustion-reforming mechanism was proposed by Prettre *et al.*[21] that the overall oxidation involves two steps, in which carbon dioxide and water are the primary products of an initial exothermic oxidation of methane, followed by the endothermic reactions of methane and two primary products (carbon dioxide and water) to produce carbon monoxide. The other mechanism is a pyrolysis mechanism that was proposed by Schmidt *et al.* that carbon monoxide is produced via the pyrolysis products of methane without the pre-formation of carbon dioxide[22]. This means that carbon monoxide and hydrogen are produced and subsequently oxidized to water and carbon dioxide.

The reaction mechanisms in the plasma are more complicated. Liu *et al.* have proposed the plasma induces oxidative coupling of methane mechanism[16]. The oxygen molecules are easily initiated to form negative ions by dissociative attachment (Reaction 5.6). The negatively charged oxygen activates a methane molecule by abstracting a hydrogen atom from the methane molecule to form the methyl radical (CH_3) in the corona discharge (Reaction 5.7). The methyl radical further combines with oxygen species to form carbon monoxide and carbon dioxide as shown in Reactions 5.8-5.15. H radical combines with another H radical to form hydrogen (Reaction 5.16). The reaction mechanism for the combination of catalyst and plasma has no clear explanation since each of mechanisms has not yet been elucidated.

$$e^- + O_2 \rightarrow 2O + e^- \rightarrow O^- + O \quad (5.6)$$

$$CH_4 + O^- \rightarrow CH_3 + OH^- \quad (5.7)$$

$$CH_3 + O \rightarrow HCHO + H \quad (5.8)$$

$$HCHO + O \rightarrow OH + CHO \quad (5.9)$$

$$CHO + O \rightarrow OH + CO \quad (5.10)$$

$$CHO + O \rightarrow CO_2 + H \quad (5.11)$$

$$HCHO + H \rightarrow H_2 + CHO \quad (5.12)$$

$$CHO + H \rightarrow H_2 + CO \quad (5.13)$$

$$HCHO + OH \rightarrow CHO + H_2O \quad (5.14)$$

$$CHO + OH \rightarrow CO + H_2O \quad (5.15)$$

$$2H \rightarrow H_2 \quad (5.16)$$

In the absence of Pt/KL, the lowest CO/C_2 ratio (Figures 5.6 and 5.7) and the highest H_2/CO ratio (Figures 5.8 and 5.9) were found at the lowest current, the highest applied frequency (700 Hz) and the lowest input low side voltage (48 V). For further increases in current, decreases in applied frequency or increases in input low side voltage, CO/C_2 and H_2/CO ratios were independent of applied frequency and input low side voltage. In the presence of catalyst, CO/C_2 and H_2/CO ratios increased with decreasing applied frequency and increasing input low side voltage. In addition, the CO/C_2 ratio in the presence of catalyst was lower than in the absence of catalyst. In the absence of Pt/KL when the applied frequency was decreased and the input low side voltage was increased, the methane and oxygen were consumed at the same rate so the reaction pathways were not changed. In the presence of Pt/KL, methane conversion increased with decreasing applied frequency and increased with input low side voltage while the oxygen conversion remained almost constant at 100% so the reaction pathway was altered.

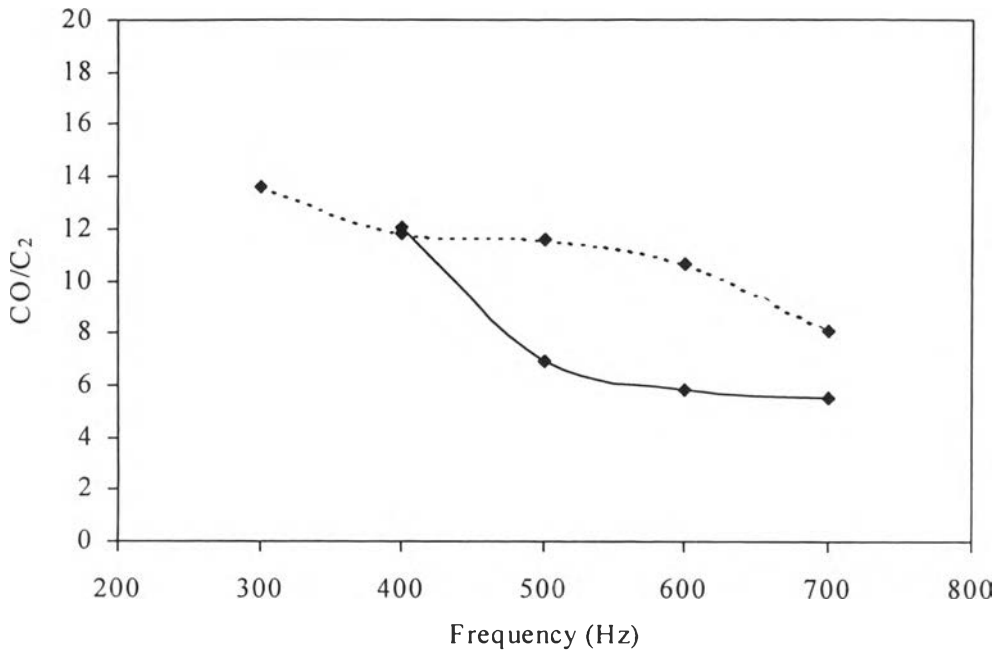

Figure 5.6 Effects of applied frequency on CO/C_2 mole ratio for methane partial oxidation in air; input low side voltage, 64 V and with (—)/without (---) Pt/KL.

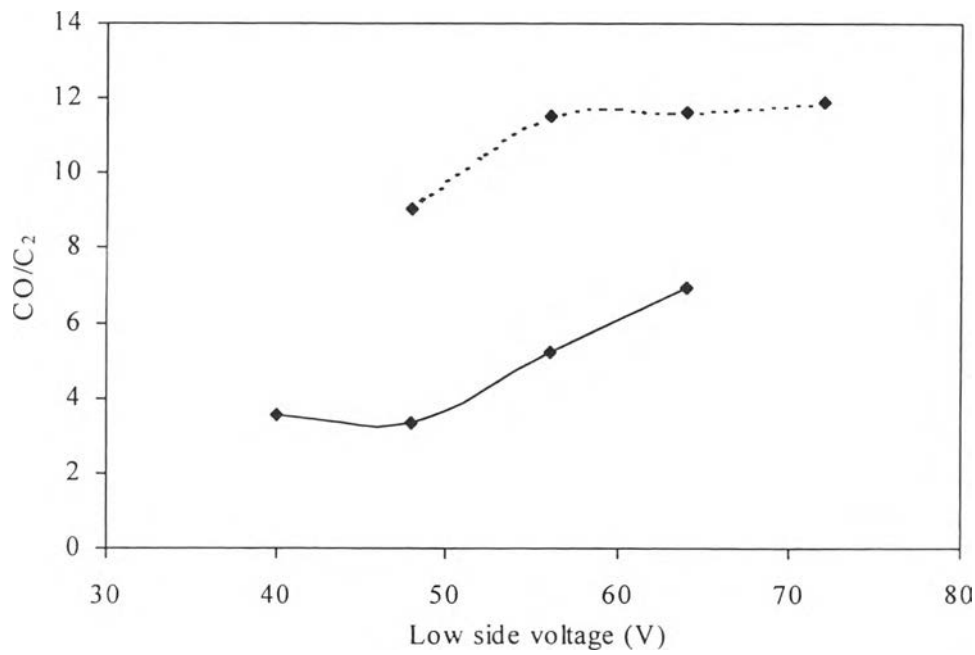

Figure 5.7 Effects of input low side voltage on CO/C_2 for methane partial oxidation in air; applied frequency, 500 Hz and with (—)/without (---) Pt/KL.

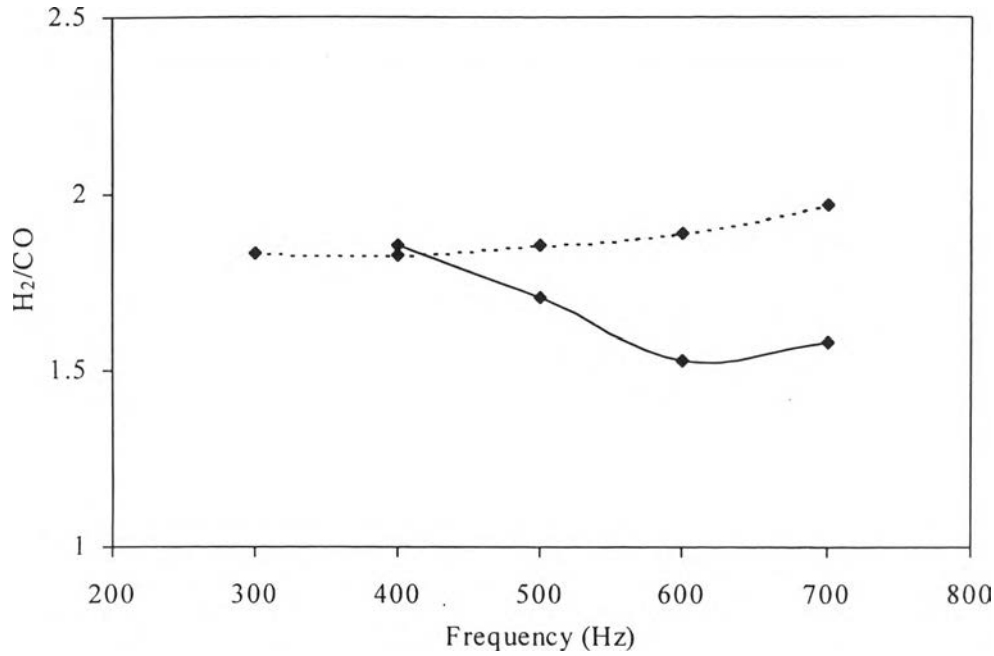

Figure 5.8 Effects of applied frequency on H_2/CO mole ratio for methane partial oxidation in air; input low side voltage, 64 V and with (—)/without (---) Pt/KL.

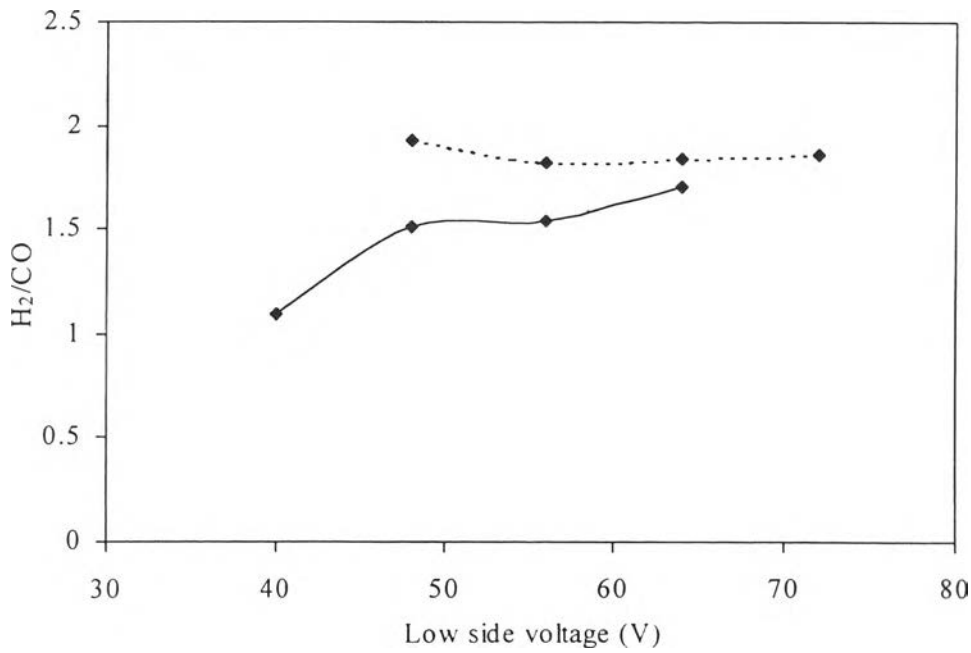

Figure 5.9 Effects of input low side voltage on H_2/CO for methane partial oxidation in air; applied frequency, 500 Hz and with (—)/without (---) Pt/KL.

As previously mentioned, partial oxidation of methane must avoid deep oxidation reactions, which produce carbon dioxide and water. However, carbon dioxide was not found in this study. The dissociative attachment of carbon dioxide can occur within the range of electron energies of corona discharges to produce CO and O^- (Reactions 5.17, 5.18)[16], therefore carbon dioxide production under electrical discharge may be lower than high temperature partial oxidation.

$$CO_2 + e^- \rightarrow CO + O^- \quad (5.17)$$

$$CO_2 + e^- \rightarrow O + CO + e^- \quad (5.18)$$

For the study of carbon dioxide reforming with methane, CO_2/CH_4 feed mole ratio was kept constant at 1:1 with 4% oxygen in feed gas. A small amount of oxygen was added to the feed gas in order to reduce the carbon formation and sustain the discharge because carbon forms easily in carbon dioxide reforming with methane.

The effects of applied frequency and input low side voltage on reactant conversions for carbon dioxide reforming with methane are shown in Figures 5.10 and 5.11, respectively. Similar to partial oxidation of methane in air, decreasing applied frequency and increasing input low side voltage enhanced the conversions of the feed gases. The conversions of methane, carbon dioxide, and oxygen increased with decreasing applied frequency and increased with input low side voltage. As already mentioned, an increase in conversion can be explained by an increase in current, as shown in Figures 5.12 and 5.13. Zhou *et al.*[8] also found that an increase in the specific input energy (electric power/flowrate) lead to an increase in the methane and carbon dioxide conversions and the production of syngas. In contrast with partial oxidation of methane in air, the conversion of each feed gas of carbon dioxide reforming with methane showed no significant difference between the presence and absence of Pt/KL because Pt/KL had no effect on current.

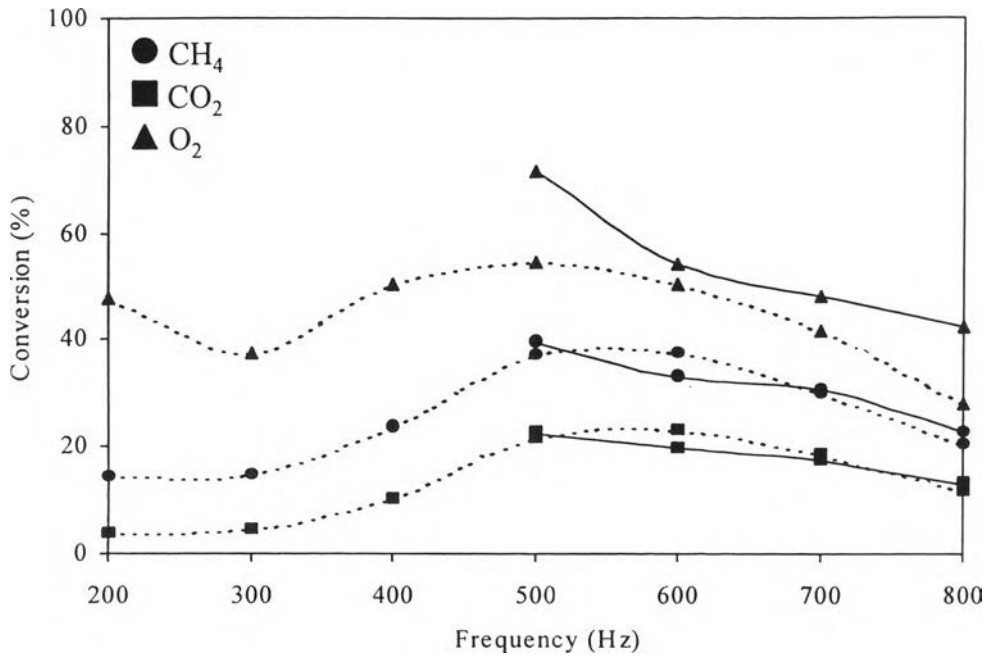

Figure 5.10 Effects of applied frequency on reactant conversions for carbon dioxide reforming with methane; input low side voltage, 56 V and with (—)/without (---) Pt/KL.

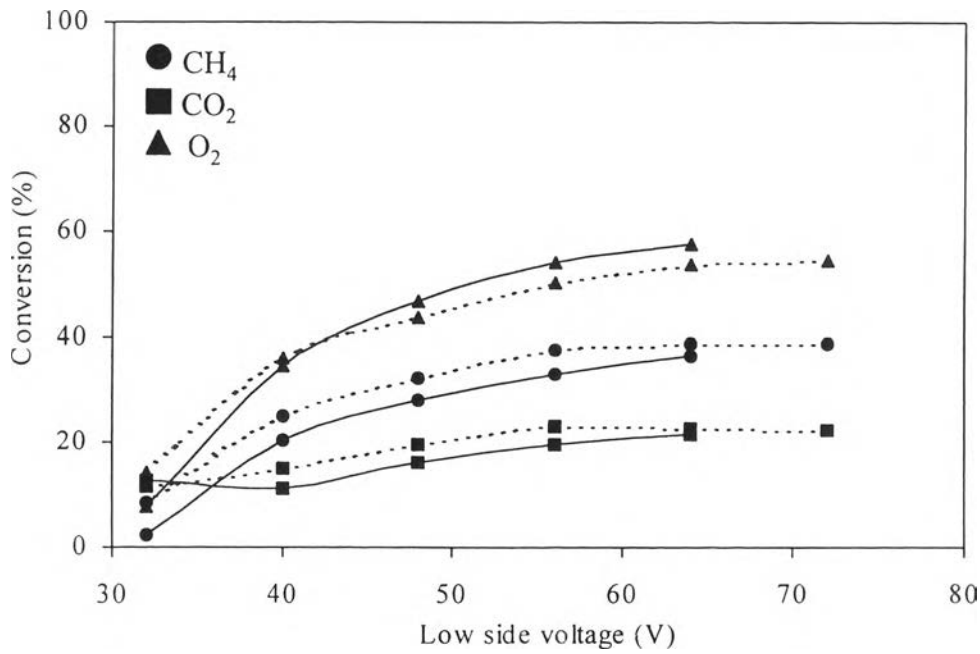

Figure 5.11 Effects of input low side voltage on reactant conversions for carbon dioxide reforming with methane; applied frequency, 600 Hz and with (—)/without(---) Pt/KL.

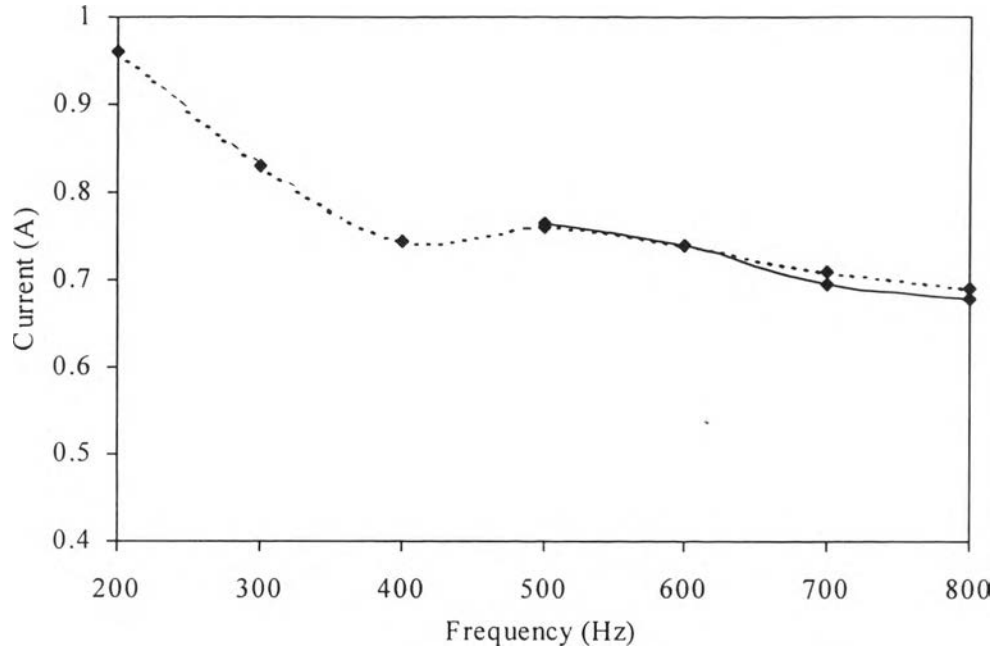

Figure 5.12 Effects of applied frequency on current for carbon dioxide reforming with methane; input low side voltage, 56 V and with (—)/without (---) Pt/KL.

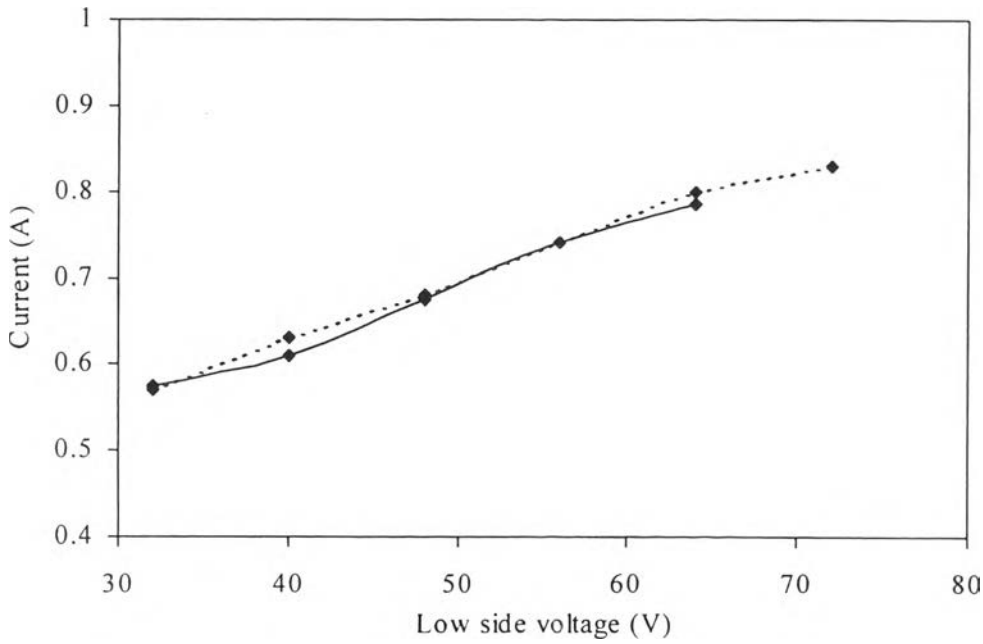

Figure 5.13 Effects of input low side voltage on current for carbon dioxide reforming with methane; applied frequency, 600 Hz and with (—)/without (---) Pt/KL.

At an input low side voltage of 32 V, methane conversion was lower than carbon dioxide conversion but methane conversion was higher than carbon dioxide at the higher input low side voltages. The same result was found using a catalytic DBD (dielectric barrier discharges) with zeolites by Eliasson *et al.*[14]. They proposed that due to the fact that carbon dioxide's dissociation energy (5.5 eV) is lower than methane's dissociation energy (~ 10 eV), carbon dioxide is easier to dissociate than methane at low input power. Increasing input power gives a higher rate of generation of active species, H, OH, O and O^-, that can interact with methane to produce methyl radicals resulting in increasing methane conversion.

From these results, it appears that the introduction of Pt/KL into the corona discharge reactor reduced the conversion of methane and carbon dioxide but increased the conversion of oxygen. Adding zeolite into the discharge gap of a DBD also reduced methane and carbon dioxide conversions in the direct conversion of methane and carbon dioxide to higher hydrocarbons[14]. In addition, carbon monoxide selectivity was slightly reduced when a zeolite was used.

All experiments in this study, except studying the effect of frequency on carbon dioxide reforming with methane without Pt/KL, were operated without carbon formation in the reactor. To study the effect of carbon formation, the frequency was varied in the range of 200-800 Hz. Figure 5.10 shows the conversions of feed gases increased with decreasing applied frequency from 800 Hz to 500 Hz. With further decreases in frequency, the conversions of methane, carbon dioxide, and oxygen decreased. However, the current increased from 0.69 to 0.96 along with the decreased applied frequency. Carbon began to form in the reactor when the applied frequency was decreased lower than 500 Hz. Since this carbon is electrically conductive, the current tends to flow almost entirely through these carbon deposits. This reduces the number of discharge streamers and limits the number of energetic electrons that can interact with the feed gases in the reaction zone resulting in lower reactant conversions as well as reaction rates. Carbon can be formed from the decomposition of methane and carbon monoxide as shown in Reactions 5.19 and 5.20. When the current was increased by decreasing the applied frequency and by increasing input low side voltage, the electron energy is high enough to initiate the decompositions of methane and carbon monoxide into carbon.

$$CH_4 \rightarrow CH_3 \rightarrow CH_2 \rightarrow CH \rightarrow C \qquad (5.19)$$

$$e^- + CO \rightarrow C + O + e^- \qquad (5.20)$$

Carbon dioxide conversion was lower than methane conversion. A similar result was found in a DBD reactor by Zhou *et al.*[8]. They explained that the carbon dioxide molecule is activated to form carbon monoxide by hydrogen atom (Reaction 5.21) which is abstracted from methane molecule and oxygen reacting with the methane molecule to form methyl radical (Reaction 5.7). The rate coefficient of Reaction 5.7 is several orders of magnitude higher than that of the Reaction 5.21. Consequently, carbon dioxide conversion is lower than methane conversion.

$$CO_2 + H \rightarrow CO + OH \qquad (5.21)$$

The CO/C_2 and H_2/CO ratios are almost constant with increasing input low side voltage and increasing applied frequency in the presence and absence of Pt/KL, as shown in Figures 5.14-5.17, since the hydrogen production rate is the same as the carbon monoxide production rate. Zhou *et al.*[8] reported that at low specific input energy, the H_2/CO ratio was almost independent on the specific input energy. It can be concluded that applied frequency and input low side voltage have no significant effect on reaction pathways of carbon dioxide reforming with methane.

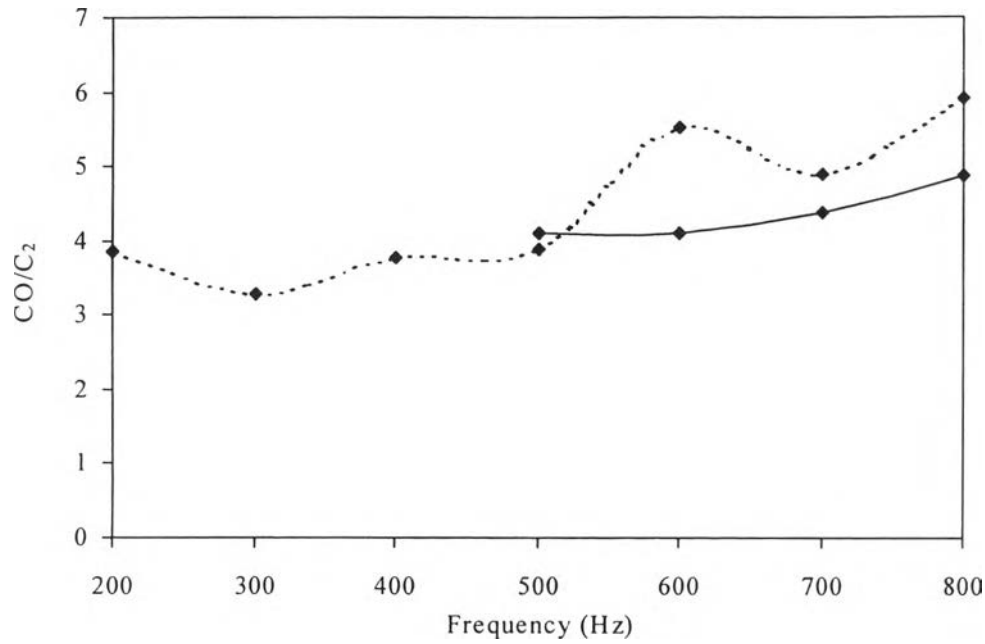

Figure 5.14 Effects of applied frequency on CO/C_2 for carbon dioxide reforming with methane; input low side voltage, 56 V and with (—)/without (---) Pt/KL.

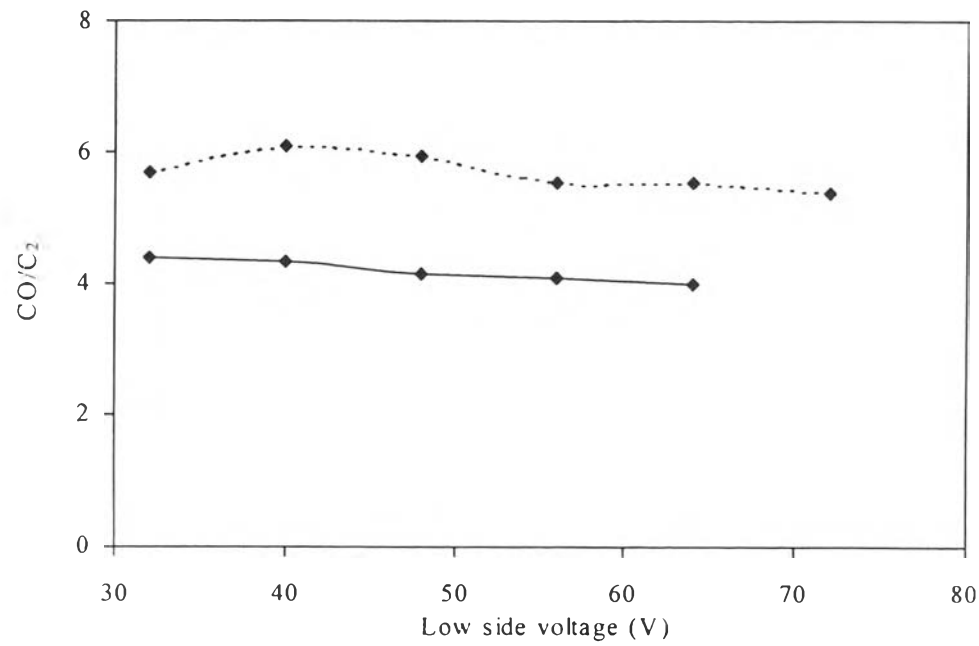

Figure 5.15 Effects of input low side voltage on CO/C_2 for carbon dioxide reforming with methane; applied frequency, 600 Hz and with (—)/without (---) Pt/KL.

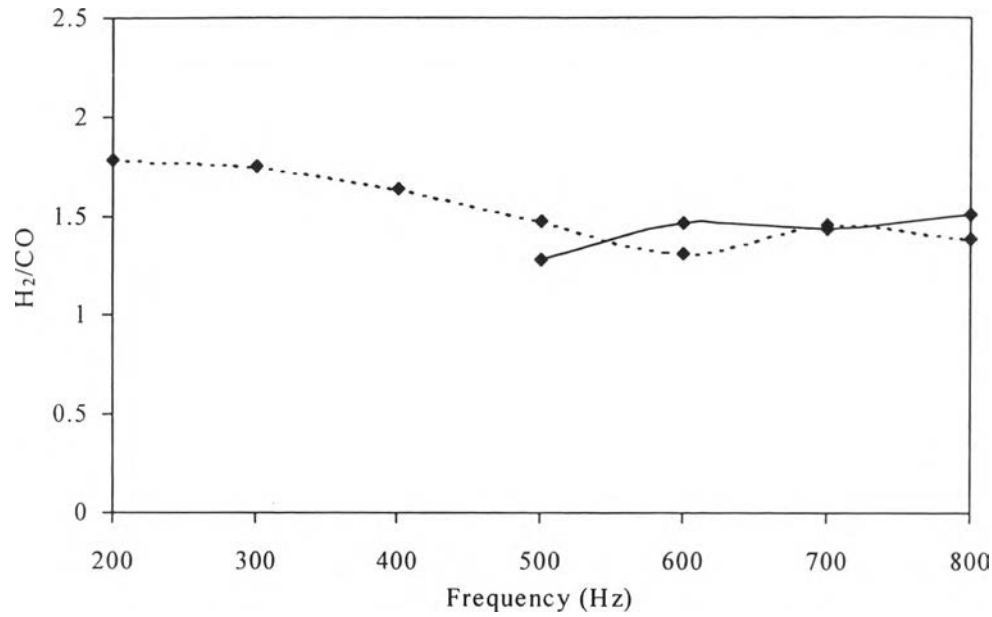

Figure 5.16 Effects of applied frequency on H_2/CO for carbon dioxide reforming with methane; input low side voltage, 56 V and with (—)/without (---) Pt/KL.

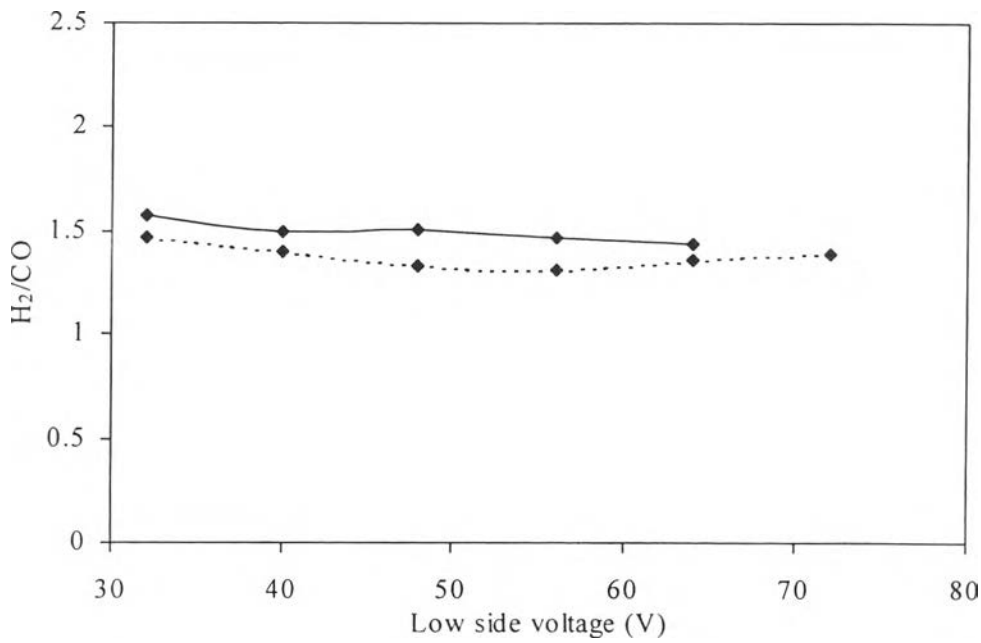

Figure 5.17 Effects of input low side voltage on H_2/CO for carbon dioxide reforming with methane; applied frequency, 600 Hz and with (—)/without (---) Pt/KL.

5.5 Conclusions

Pt/KL catalyst showed a difference between partial oxidation of methane and carbon dioxide reforming with methane in a corona discharge reactor. Decreasing applied frequency and increasing input low side voltage in the absence and presence of Pt/KL could enhance both partial oxidation of methane and carbon dioxide reforming with methane by increasing reactant conversions, except in the case of partial oxidation of methane in the presence of Pt/KL. In that case, all oxygen molecules were consumed and this limited methane conversion and impacted the product distribution. In the presence of the catalyst, carbon formation was more significant at both electrodes due to the rough surface of the catalyst. For partial oxidation of methane in the absence of Pt/KL at high current, the CO/C_2 and H_2/CO ratios were not dependent on applied frequency and input low side voltage, but in the presence of Pt/KL, the CO/C_2 and H_2/CO ratios increased with decreasing applied frequency and increased with input low side voltage. The present results demonstrate that the combination of catalyst and corona discharge gave a higher oxygen conversion, while the methane conversion was lower for the partial oxidation of methane, though this combination had no strong effect on carbon dioxide reforming with methane.

5.6 Acknowledgement

The Thailand Research Fund is gratefully acknowledged for supporting this research work as well as providing a scholarship for the first author.

5.7 References

1. Walker, A.V.; King, D.A. *J. Phys. Chem. B* **2000**, 104, 6462-6467.
2. O'Connor, M.A.; Julian J.H.R. *Catal. Today* **1998**, 46, 203-210.
3. Larkin, D.W.; Caldwell, T.A.; Lobban, L.L.; Mallinson, R.G. *Energy and Fuels* **1998**, 12, 740-744.

4. Larkin, D.W.; Leethochawalit, M.; Chavadej, S.; Caldwell, T.A.; Lobban, L.L.; Mallinson, R.G. "Carbon Pathways, CO_2 Utilization, and In Situ Product Removal in Low Temperature Plasma Methane Conversion to Methanol," *Proc. 4th Int. Conf. on Greenhouse Gas Control Technologies, Interlaken, Switzerland*, **1998**, 397-402.
5. Larkin, D.W.; Lobban, L.L.; Mallinson, R.G. *Ind. Eng. Chem. Res.* **2001**, 40 (7), 1594-1601.
6. Thanyachotpaiboon, K.; Chavadej, S.; Caldwell, T.A.; Lobban, L.L.; Mallinson, R.G. *AIChE J.* **1998**, 44(10), 2252-2257.
7. Yao, S.L.; Takemoto, T.; Ouyang, F.; Nakayama, A.; Suzuki, E. *Energy and Fuels* **2000**, 14(2), 459-463.
8. Zhou, L.M.; Xue, B.; Kogelschatz, U.; Eliasson, B. *Energy and Fuels* **1998**, 12, 1191-1199.
9. Zhou, L.M.; Xue, B.; Kogelschatz, U.; Eliasson, B. *Plasma Chem. Plasma Proc.* **1998**, 18(3), 375-393.
10. Lesueur, H.; Czernichowski, A.; Chapelle, J. *Int. J. Hydrogen Energy* **1994**, 1 (2), 139-144.
11. Lowke, J.J.; Morrow, R. *Pure&Appl. Chem.* **1994**, 66, 1287-1294.
12. Chang, J.-S.; Lawless, P.A.; Yamamoto, T. *IEEE Trans. Plasma Sci.* **1991**, 19, 1152-1165.
13. Liu, C.-J.; Mallinson, R.G.; Lobban, L.L. *J. Catal.* **1998**, 179, 326-334.
14. Eliasson, B.; Liu, C.-J.; Kogelschatz, U. *Ind. Eng. Chem. Res.* **2000**, 39, 1221-1227.
15. Okazaki, K.; Hirai, S.; Nozaki, T.; Ogawa, K.; Hijikata, K. *Energy* **1997**, 22 (2/3), 369-374.
16. Liu, C.; Marafee, A.; Hill, B.; Xu, G.; Mallinson, R.G.; Lobban, L.L. *Ind. Eng. Chem. Res.* **1996**, 35, 3295-3301.
17. Hill, B.J. Master Thesis, University of Oklahoma, 1997.
18. Morinaga, K.; Suzuki, M. *Bull. Chem. Soc. of Japan.* **1961**, 34(2), 157-161.
19. Morinaga, K.; Suzuki, M. *Bull. Chem. Soc. of Japan.* **1962**, 35(2), 204-207.
20. Hu, Y.H.; Ruckenstein, E. *J. Phys. Chem. A* **1998**, 102, 10568-10571.
21. Prettre, M.; Eichner, C.; Perrin, M. *Trans. Faraday Soc.* **1946**, 42, 335-340.

22. Torniainen, P.M.; Chu, X.; Schmidt, L.D. *J. Catal.* **1994**, 146, 1-10.